Efficient-Nets and their Fuzzy Ensemble: An Approach for Skin Cancer Classification

Dibyendu Das[1], Nikhilanand Arya[2,*[0000−0002−2821−2051]], and Sriparna Saha[2[0000−0001−5458−9381]]

[1] Ramakrishna Mission Vivekananda Educational and Research Institute Belur , Howrah, India
dsdibyendu7@gmail.com
[2] Indian Institute of Technology Patna, Bihar, India
nikhilanand_1921cs24@iitp.ac.in
sriparna@iitp.ac.in

Abstract. Skin cancer is common and deadly among all cancer types, and its increasing cases in the last decade have put tremendous stress on dermatologists. With the advancement in medical imaging techniques, dermoscopic visual inspection with proper training of dermatologists can achieve approximately 80 percent diagnostic accuracy. However, in real-life scenarios, most dermatologists ignore the procedural algorithms (3-point checklist, ABCD rule, Menzies method, 7-point checklist) and follow their experience-based instincts. It raises the need for automated dermoscopy diagnosis, and this paper proposes a novel Choquet Fuzzy Ensemble of reward penalized Efficient-Nets for multi-class skin cancer classification. The base classifiers of the architecture are trained with the novel macro F1_score-based rewarding technique to handle the class imbalance of International Skin Imaging Collaboration (ISIC) data. After that, we combine the prediction probabilities of base classifiers using Choquet fuzzy integral to get the final predicted labels. The proposed architecture is evaluated based on ISIC multi-class skin cancer classification. The rewarded cross-entropy loss-based training regime showcased its superiority over weighted cross entropy loss training by attaining 2.61%, 3.06%, and 2.65% improvements in balanced accuracies of base classifiers. The proposed ensemble also outperforms the existing state-of-the-arts in terms of performance. Our model's highest balanced accuracy (88.15%) over its base classifiers and the state-of-the-art makes our model efficient and trustworthy in the classification goal.

Keywords: Skin cancer · Ensemble learning · Choquet fuzzy Integrals · Reward function.

1 Introduction

A study on skin cancer by the American Cancer Society (ACS) [1] suggests a enormous increase in skin cancer cases globally. If we see the figures, non-

* Corresponding author and having equal contribution with the first author

melanoma skin cancer contributes to 2-3 million and melanoma skin cancer accounts for 132,000 cases globally each year. The ACS has an estimated 97,220 situ (noninvasive) melanoma, confined to the epidermis, and 99,780 invasive melanoma, spread to the dermis, resulting in 197,700 cases of melanoma in the U.S. only. The past decade (2012-2022) has observed a 31% shoot up in new invasive melanoma cases diagnosed annually. The occurrence of skin cancer is perturbing, as every three cancer diagnoses have one skin cancer. Americans are very susceptible to it because one in five Americans will have skin cancer at some point in their lives. If we analyze the statistics of melanoma deaths, 7,650 people will die of melanoma in 2022, which is an increase of 6.5% from last year. Although melanomas occurrences are low (<5%) among all skin cancers in the United States, 75% of all skin cancer-related deaths correspond to melanomas. The sharp decline in the 5-year survival rate from 99% to 14% between early and late detection of melanoma shows the criticality of early-stage detection. Shifting our view from uncommon but more catastrophic melanoma [13] to common and less fatal keratinocyte cancer such as squamous cell carcinomas (including actinic keratoses and Bowen's disease) and basal cell carcinomas shows the highest economic burden for Medicare patients [1].

The surge in skin cancer cases and shortage of dermatologists per capita [10] establishes the fact that there is a dire need for automated dermatology to eliminate the human intervention for the assessment of dermoscopic images [3]. Medical practitioners and patients can proactively track skin lesions and detect cancer earlier. It may benefit the patients by reducing economic expenses and can be a life savior with early-stage detection. The automated system may be helpful for the clinician as well by reducing the manual overhead.

2 Related Works

An artificial intelligence (AI) based automated system requires a plethora of data for learning, and from a data perspective, an earlier effort to create a public archive of very few images was made [3, 12]. Too small dataset lacks the incorporation of multi-class classification tasks and compromises the generalization ability of the AI architectures. In recent years, the ISIC* has begun to aggregate a large-scale publicly accessible dataset of more than 33,000 dermoscopic images from leading clinical centers internationally. A look into the past literature on automated skin cancer classification using dermoscopic images shows several works. *Codella et. al.* [5] have used 5248 dermoscopy images of melanoma (334), atypical nevi (144), and benign lesions (2146) by combining deep learning, sparse coding, and support vector machine (SVM) learning algorithms for melanoma vs. non-melanoma lesions, and melanoma vs. atypical lesions identification. Previous studies of image analysis using deep learning in skin cancer detection have been drawn to dermatologists' attention [8, 9, 11]. In the work of *Dascalu and David* [8], dermoscopy images acquired from a skin

* https://challenge.isic-archive.com/data/

magnifier with polarized light were sonified to audio outputs by a deep learning (DL) algorithm, and the audios were further analyzed by a secondary DL for benign and malignant classification of skin lesions. The convolutional neural network (CNN) is one of the deep learning methods with the potential to analyze general and highly variable tasks in dermoscopic images. *Li and Shen* [11] used the ISIC2017 dataset [6] and proposed a deep learning framework consisting of two fully convolutional residual networks (FCRN) and a straight-forward CNN for lesion segmentation, lesion classification, and lesion dermoscopic feature extraction tasks, respectively. *Kassani and Kassani* [9] have used the ISIC2018 dataset [6, 20] to analyze the performance of several state-of-the-art convolutional neural networks and selected ResNet50 as the best CNN in dermoscopic images classification.

The efficacy of CNNs in recent research motivated us to design our novel architecture for eight-class skin cancer classification tasks using ISIC2018 [6,20], ISIC2019 [6, 7, 20], and ISIC2020 [15] data. The proposed work is also inspired by the success of classifier ensembling techniques to improve the classification accuracy of the individual classifiers [2, 14]. The proposed architecture uses ensemble of three Efficient-Nets (B4, B5 and B6) motivated by the top performing architecture of ISIC2019 challenge's leader-board. The existing state-of-the-art architecture is the ensemble of all Efficient-Nets (B0 to B6) where B4, B5 and B6 are the best performing models in terms of balanced accuracies. The contributions of this study are as follows:

- We propose the new Macro-F1 Score-based reward function algorithm for training base classifiers (specifically, Efficient-Nets). It makes the model more robust for the class imbalance data.
- We propose a Choquet Fuzzy Integral based ensemble of base classifiers, which utilizes the probabilistic outcomes of each classifier to get the final prediction.

3 Dataset

The dataset used in this study is sourced from ISIC Archive, but we have downloaded it from Kaggle (SIIM-ISIC Melanoma Classification)*. The Kaggle repository consists of dermoscopy images from ISIC2018, ISIC2019, and ISIC2020 resulting in a total of 57964 images, out of which 25272 belong to ISIC2018-19 and 32692 belong to ISIC2020. We have utilized the JPEG version of these images with uniform sizes 512× 512 for our study. The dataset is categorized into eight different types of skin cancers as Melanoma (MEL), Melanocytic Nevus (NV), Basal cell carcinoma (BCC), Actinic Keratoses (AK), Benign Keratosis (BKL), Dermatofibroma (DF), Vascular Lesion (VASC), and Squamous cell carcinoma (SCC). These target classes are directly available for ISIC2018-19 data, but for the categorization of ISIC2020 data, we have used the diagnosis column from the metadata file. The un-categorized samples from the dataset are mapped to

* https://www.kaggle.com/c/siim-isic-melanoma-classification

separate unknown (UNK) classes, and we have discarded these samples from our study along with the redundant instances, resulting in 31265 images as a final dataset. The classwise distribution of the data is depicted in Fig 1.

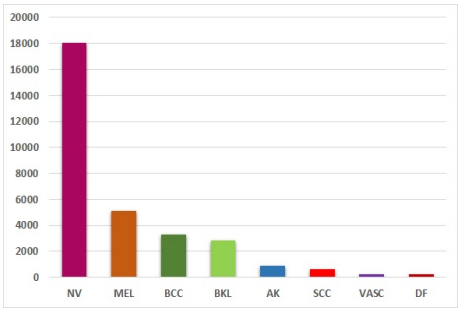

Fig. 1: Class-wise data distribution of ISIC(2018,2019,2020) skin cancer training data where x and y axes represents eight different types of skin cancers and respective image counts in the dataset, respectively.

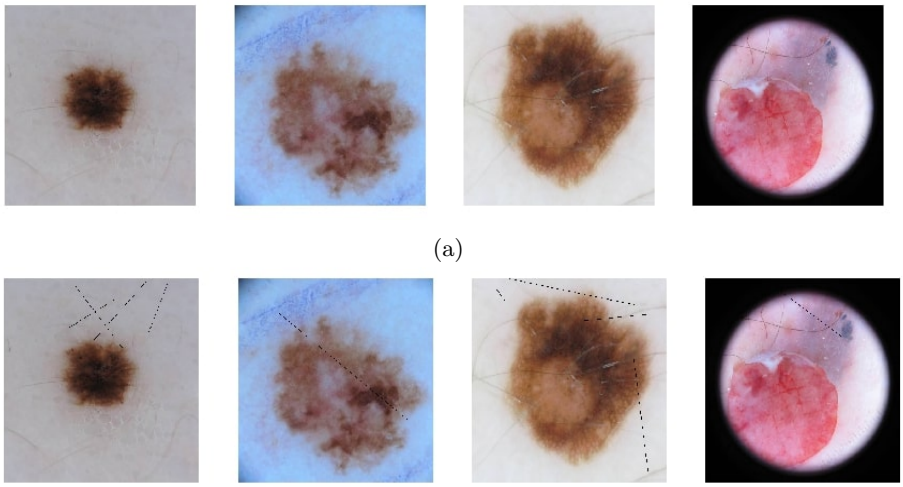

(a)

(b)

Fig. 2: (a) Some original dermoscopic images of skin cancer without hair insertion and (b) Skin cancer dermoscopic images with hair insertion using Buffon's needle concept.

The data is further divided into a train-test (80:20) set for training and testing the model, and 15% of the training set is selected as validation data. Most of the dermoscopic lesion images in the data portray overlapping body hair with the lesion region, and several hair-removal techniques have been suggested. Some issues, such as how to interpolate overlapping parts, remained, nevertheless. We

thus use a different strategy by enhancing the fake body hairs to images using Buffon's needle [4] as the foundation. A sample representation of artificial hair insertion can be visualized from Fig. 2a and 2b.

The generalization and robustness are the primary traits of any AI architecture. We have incorporated some pre-processing steps to the train data during training to maintain these traits. It includes random application of various image transformation techniques such as transpose, flip, rotate, random brightness, random contrast, motion blur/ median blur/Gaussian blur/Gauss noise, Optical distortion/grid distortion/elastic transform, CLAHE, hue saturation value, shift scale rotate, cutout, and normalize.

4 Methods

The proposed architecture is the Choquet fuzzy integral [16] ensemble of three different EfficientNets (B4, B5, and B6) [18] with a reward function penalization for miss-classifications, and it is depicted in Fig 3 and 4, respectively.

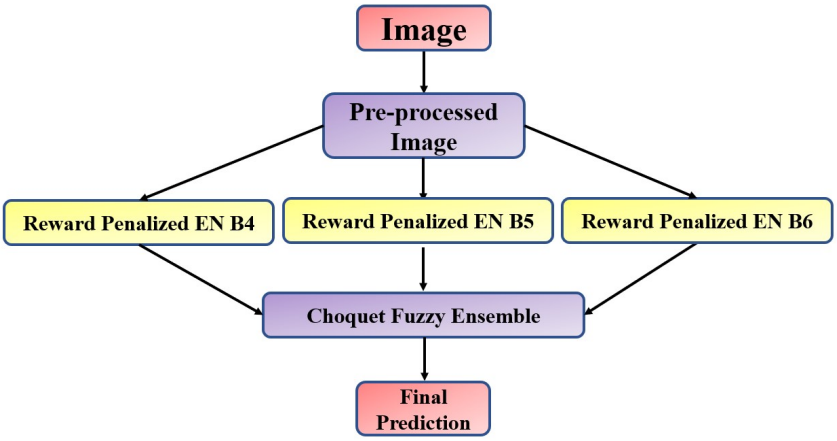

Fig. 3: The proposed architecture: Choquet Fuzzy Ensemble of Reward Penalized Efficient-Nets (EN) B4, B5 and B6.

The data is highly class imbalanced and can be seen from Fig. 1. So, we have performed weighted random sampling in each training batch to over-sample the minority classes. The best three EfficientNets (B4, B5, and B6) are selected after training and evaluating the balanced test accuracy of all possible EfficientNets on the final test data. The training of Efficient-Nets is performed separately in a five-fold stratified cross-validation framework with the proposed reward function and the best model from each fold is selected. We have averaged the performance of best models from each fold to get the final evaluation measure over test data.

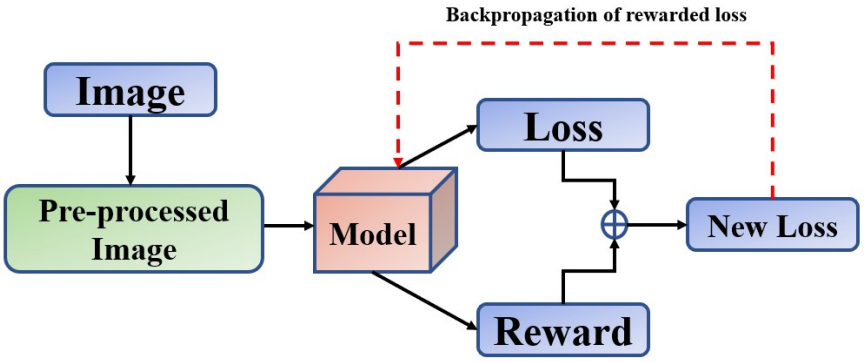

Fig. 4: The reward function workflow for the base classifier.

The average softmax outcomes from each Efficient-Net, representing the class probabilities of eight different skin cancer classes, are ensemble with Choquet fuzzy integral for final classification results. The reward function and Choquet fuzzy integral are further explained in subsections 4.1 and 4.2.

4.1 Reward Function

In this section, we propose a novel rewarding algorithm to handle the class imbalance of the ISIC skin cancer dataset being used in this study.

Algorithm 1 Algorithm for Reward Function

Input: Batches from Train Dataloader
Output: Penalized Loss
Setting :
Class $= \{c_1, c_2, \cdots, c_T\}$, Batch_size $= l$, loss_fun $=$ loss()
Training_Data $= \{(x_i, y_i) \ : \ i = 1(1)n, \ y_i \in Class\}$
Batch $= \{\{(x^{(j)}, y^{(j)}) \ : \ j = 1(1)l\}_k \ : \ k = 1(1)[n/l]\}$
model $=$ model()
for item in Batch **do**
  input $= \{x^{(j)} \ : \ j = 1(1)l\}$
  label $= \{y^{(j)} \ : \ j = 1(1)l, \ y^j \in Class\}$
  $\{\hat{y}^{(j)} \ : \ j = 1(1)l\}$ = model(input)
  calculate Precison P_t,and Recall R_t for each $t \in Class$
  Macro-F1_Score $= \frac{1}{|Class|} \sum \frac{2P_t R_t}{P_t + R_t}$
  Reward $= \frac{1}{Macro-F1\_Score+\epsilon}$
  loss $=$ loss _fun (output, label)
  Penalized_loss $=$ loss $+$ Reward
end for

To handle the class imbalance, we have used the concept of reinforcement learning [19] which suggests that whenever a model makes any mistake, it learns from it. We know that the Macro-F1_score measures the class-wise importance. For that reason, we have introduced a reward function as inverse of Macro-F1_score. We have calculated Macro-F1_score for each batch. For some batches, it could be zero, in that case, an epsilon is added. The reward is then incorporated with the loss function of the model to penalize or reward the incorrect and correct classifications, respectively. The detailed implementation is presented in Algorithm 1. The rewarding technique is not an overhead in terms of complexity as the reward penalization is performed for each item present in the train batch during training with batch size l, as given in the algorithm. It adds up only linear complexity for the calculation of Macro-F1_score and respective rewarded loss if compared to the complexity of non-rewarded loss calculation.

4.2 Ensemble: Choquet Fuzzy Integral

In this research, we suggest an integration of several classifiers using fuzzy fusion to make use of the ascendancy of separate Efficient-Net classifiers rather than a single one. The input of the fuzzy fusion is directly regarded as the confidence ratings from several classifiers. The uncertainty of the decision scores is a piece of extra information from a classifier harnessed by the fusion strategy. For our work, we formulated the problem as follows.
Problem Formulation:

- Let C_j denotes the $\mathrm{j_{th}}$ model, where j=1,2,$\cdots$,M.
- acc_j be the test accuracy for the $\mathrm{j_{th}}$ model.
- Test set
  $(D_{Test}) = \{(x^{(i)}, y^{(i)}) \ : \ x^{(i)} \in \mathbf{R}^{C\times W\times H}, y^{(i)} \in \mathbf{R}^d, i = 1(1)n\}$.
  Here C, W and H represents the Channel, Width and Height of the input image, $x^{(i)}$, d is the number of classes.
- V(.) = Measure of consistency of a classifier $\in$ [0,1] and calculated as:
  $V(C_i) = (acc_i)/(\sum_{i=1}^{M} acc_i)$. If S is the set of all classifiers, then V(S) = 1 indicates that the classifier can be trusted and that its findings are consistent, but $V(\phi) = 0$ indicates that the classifier cannot be trusted.
- Here, we assume that for any two classifiers they are capturing different views of a dataset, so if C_1 and C_2 are two classifiers then in mathematical form $C_1 \cap C_2 = \phi$ and from theory of fuzzy integral [17] we can find a Fuzzy measure, $\lambda > -1$ in such a way that we can estimate the importance of two models together in following way:

$$V(C_1 \cup C_2) = V(C_1) + V(C_2) + \lambda V(C_1)V(C_2) \tag{1}$$

- **Definition of Choquet Fuzzy Integral :** Suppose μ is the fuzzy measure on $\mathcal{F}$, a collection of subsets of S. The Choquet fuzzy integral of the function

mapping: $h : \mathcal{F} \rightarrow \mathcal{R}$ with relation to μ is explained by:

$$Ch_{\mu}(h) = \sum_{i=1}^{M} h_{(i)}[\mu(A_{(i)}) - \mu(A_{(i+1)})] \tag{2}$$

Here, i is the subset size, $h_{(1)} \leq h_{(2)} \leq \cdots \leq h_{(M)}$. Moreover $A_{(i)} = i, \cdots, n, A(n+1) = \phi$

Now, we have to calculate the λ using the following equation:

$$1 + \lambda = \prod_{i=1}^{M} (\lambda V(C_i) + 1) \tag{3}$$

For each input image $x^{(i)}$ corresponding to model C_j, we have the prediction for d different classes as $\hat{Y_i}^j = (\hat{y}^j_{i,1}, \hat{y}^j_{i,2}, \cdots, \hat{y}^j_{i,d})$. We combine these outputs from each model with corresponding model importance and define $X = (X_1, X_2, \cdots, X_d)$, where $X_k = (\hat{y}^j_{i,k}, V(C_j))$ for all $j = 1, 2, \cdots, M$.

Further, we reorder each X_k in descending order based on $\hat{y}^j_{i,k}$ values. Let, $\hat{\hat{Y}}_i = (y_1, y_2, \cdots, y_d)$ be the ensemble output with respect to $x^{(i)}$. After finding X_k ,we need to find the ensemble output $y_k \in \hat{\hat{Y}}_i$ with the help of Algorithm 2.

Algorithm 2 Algorithm for construction of final Prediction

Input: $X = (X_1, X_2, \cdots, X_d)$
Output: Final Prediction
Setting : $X_k = (\hat{y}^j_{i,k}, V(C_j)) \; \forall \; j = 1, \cdots, M$ & $x^{(i)}$.
for *Each* X_k **do**
  for $j = 1, 2, \cdots, M$ **do**
    $f_{cur} = f_{prev} + X_k[j][1] + \lambda f_{prev} X_k[j][1]$
    $pred = pred + X_k[j][0](f_{cur} - f_{prev})$
    $f_{prev} = f_{cur}$
  end for
  $y_k = \text{pred} \in \hat{\hat{Y}}_i$
end for
$\hat{y}_i \leftarrow \text{argmax}(\hat{\hat{Y}}_i)$

Thus through fuzzy integrals, the robustness is experimentally found to be higher as compared to the previously obtained normalized softmax probabilities. From the algorithm 2, it is clear that the final prediction of any given input $x^{(i)}$ is calculated with the help of softmax probabilities of all possible, d classes obtained by each of the M different base classifiers. Hence, the proposed choquet fuzzy ensemble has the complexity of $\mathcal{O}(d \times M)$.

5 Results

This section establishes the efficacy of the proposed reward function and Choquet Fuzzy ensemble.

Table 1: Comparative results of Efficient-Nets (ENs) in different training setups.

Model	***Balanced Accuracy (%)***		
	Rewarded Loss	***Non-Rewarded Loss***	***Weighted Loss***
EN B4	**87.37**	84.76	86.64
EN B5	**87.51**	84.45	86.88
EN B6	**86.62**	83.97	85.53

From Table 1, we can observe that the proposed reward function is superior over non-rewarded loss and weighted loss. The weighted cross entropy loss is the popular state-of-the art to tackle the class imbalance and it has been frequently used in top architectures of ISIC-2019 challenge. Inclusion of our proposed reward function in the training of Efficient-Nets shows 2.61%, 3.06%, and 2.65% improved balanced accuracies over non-rewarded loss; 0.73%, 0.63%, and 1.29% improvement over weighted loss for Efficient-Nets B4, B5 and B6, respectively. Following the efficacy of "with reward function training", we select these models as base classifier for our final ensemble.

Table 2: Comparative results of our proposed ensemble with state-of-the-art for skin cancer classification.

Model	**Balanced Accuracy (%)**	
	Rewarded Loss	**Non-Rewarded Loss**
Choquet Fuzzy Ensemble	**88.15**	85.17
Average Ensemble	87.80	85.02
ISIC-2019 Leaderboard: Rank 1	87.68	

To showcase the efficacy of our proposed Choquet Fuzzy Ensemble over a simple (average) ensemble and existing state-of-the-art (Top performer of ISIC-2019 Challenge Leaderboard titled "Skin Lesion Classification Using Loss Balancing and Ensembles of Multi-Resolution EfficientNets")[*], we analyze the results of these two using the same training strategies mentioned earlier. From Table 2, it is evident that the Choquet Fuzzy ensemble outperforms the average ensemble

[*] https://challenge.isic-archive.com/leaderboards/2019/

and existing state-of-the-art results in multi-class skin cancer classification. The proposed ensemble outperforms the average ensemble and ISIC-2019 Leaderboard: Rank 1 by 0.35% and 0.47% for "with reward function training" setup. If we further compare the balanced accuracies of Choquet fuzzy ensemble from table 2 and base classifier Efficient-Nets (B4, B5, and B6) from table 1 in reward function training setup, then there is performance improvement of 0.78%, 0.64%, and 1.53%, respectively. Our proposed model achieves better performance than the existing techniques because of its two main components: (1) rewarding process, which improves the model's generalization capability by penalizing in case of wrong predictions and rewarding in case of correct predictions. It stops our models from being biased towards the majority classes. (2) the Choquet Fuzzy ensemble of these rewarded/penalized base classifiers does not give equal importance to all the classifiers. Instead, it prioritizes them based on their membership value derived using Choquet Fuzzy integral.

6 Conclusion and Future Work

We conclude this study with the novel Choquet Fuzzy ensemble of Efficient-Nets in a reward function training setup. The proposed architecture showcases its superiority over the base classifiers and simple ensemble technique in multi-class skin-cancer classification. The inclusion of reward function in the training regime has helped the model learn better about the minority class and handled the critical class imbalance issue of the data. The Choquet Fuzzy ensemble of EfficientNets and its proven efficacy over a simple ensemble for dermoscopic diagnostic can be helpful for dermatologists and patients in the early detection of skin cancer. It may help reducing the burden of increasing skin-cancer cases by rapid diagnosis and also reduce the economic burden of the patients.

In the future, researchers can use additional sources of information coming from clinical investigations and demographic details of the patients to develop multi-modal architectures for skin cancer classification. Further, deep learning-based architectures can be developed to predict the type of skin cancer using mobile camera images instead of dermoscopic images to ease the diagnosis for patients and dermatologists.

Acknowledgments

Dr. Sriparna Saha gratefully acknowledges the Young Faculty Research Fellowship (YFRF) Award, supported by Visvesvaraya Ph.D. Scheme for Electronics and IT, Ministry of Electronics and Information Technology (MeitY), Government of India, being implemented by Digital India Corporation (formerly Media Lab Asia) for carrying out this research.

References

1. Cancer facts and figures 2022. american cancer society. Available: https://www.cancer.org/content/dam/cancer-org/research/cancer-facts-and-statistics/annual-cancer-facts-and-figures/2022/2022-cancer-facts-and-figures.pdf.
2. Arya, N., Saha, S.: Multi-modal classification for human breast cancer prognosis prediction: Proposal of deep-learning based stacked ensemble model. IEEE/ACM Transactions on Computational Biology and Bioinformatics **19**(2), 1032–1041 (2022). https://doi.org/10.1109/TCBB.2020.3018467
3. Barata, C., Ruela, M., Francisco, M., Mendonca, T., Marques, J.S.: Two Systems for the Detection of Melanomas in Dermoscopy Images Using Texture and Color Features. IEEE Systems Journal **8**(3), 965–979 (Sep 2014). https://doi.org/10.1109/JSYST.2013.2271540, http://ieeexplore.ieee.org/document/6570764/
4. Buffon, G.L.L.D.: Essai d'arithm´etique morale (1777)
5. Codella, N., Cai, J., Abedini, M., Garnavi, R., Halpern, A., Smith, J.R.: Deep Learning, Sparse Coding, and SVM for Melanoma Recognition in Dermoscopy Images. In: Zhou, L., Wang, L., Wang, Q., Shi, Y. (eds.) Machine Learning in Medical Imaging, vol. 9352, pp. 118–126. Springer International Publishing, Cham (2015). https://doi.org/10.1007/978-3-319-24888-2_15, http://link.springer.com/10.1007/978-3-319-24888-2_15
6. Codella, N.C.F., Gutman, D., Celebi, M.E., Helba, B., Marchetti, M.A., Dusza, S.W., Kalloo, A., Liopyris, K., Mishra, N., Kittler, H., Halpern, A.: Skin lesion analysis toward melanoma detection: A challenge at the 2017 International symposium on biomedical imaging (ISBI), hosted by the international skin imaging collaboration (ISIC). In: 2018 IEEE 15th International Symposium on Biomedical Imaging (ISBI 2018). pp. 168–172. IEEE, Washington, DC (Apr 2018). https://doi.org/10.1109/ISBI.2018.8363547, https://ieeexplore.ieee.org/document/8363547/
7. Combalia, M., Codella, N.C.F., Rotemberg, V., Helba, B., Vilaplana, V., Reiter, O., Carrera, C., Barreiro, A., Halpern, A.C., Puig, S., Malvehy, J.: BCN20000: Dermoscopic Lesions in the Wild. arXiv e-prints arXiv:1908.02288 (Aug 2019)
8. Dascalu, A., David, E.O.: Skin cancer detection by deep learning and sound analysis algorithms: A prospective clinical study of an elementary dermoscope. EBioMedicine **43**, 107–113 (May 2019). https://doi.org/10.1016/j.ebiom.2019.04.055
9. Hosseinzadeh Kassani, S., Hosseinzadeh Kassani, P.: A comparative study of deep learning architectures on melanoma detection. Tissue and Cell **58**, 76–83 (Jun 2019). https://doi.org/10.1016/j.tice.2019.04.009, https://linkinghub.elsevier.com/retrieve/pii/S0040816619300904
10. Kimball, A.B., Resneck, J.S.: The US dermatology workforce: a specialty remains in shortage. Journal of the American Academy of Dermatology **59**(5), 741–745 (Nov 2008). https://doi.org/10.1016/j.jaad.2008.06.037
11. Li, Y., Shen, L.: Skin Lesion Analysis towards Melanoma Detection Using Deep Learning Network. Sensors (Basel, Switzerland) **18**(2), E556 (Feb 2018). https://doi.org/10.3390/s18020556
12. Mendonca, T., Ferreira, P.M., Marques, J.S., Marcal, A.R.S., Rozeira, J.: PH^2 - A dermoscopic image database for research and benchmarking. In: 2013 35th Annual International Conference of the IEEE Engineering in Medicine and Biology Society (EMBC). pp. 5437–5440.

IEEE, Osaka (Jul 2013). https://doi.org/10.1109/EMBC.2013.6610779, http://ieeexplore.ieee.org/document/6610779/
13. Meyskens, F.L., Mukhtar, H., Rock, C.L., Cuzick, J., Kensler, T.W., Yang, C.S., Ramsey, S.D., Lippman, S.M., Alberts, D.S.: Cancer Prevention: Obstacles, Challenges, and the Road Ahead. JNCI: Journal of the National Cancer Institute **108**(2) (Feb 2016). https://doi.org/10.1093/jnci/djv309, https://academic.oup.com/jnci/article-lookup/doi/10.1093/jnci/djv309
14. Paul, S., Saha, S., Singh, J.P.: COVID-19 and cyberbullying: deep ensemble model to identify cyberbullying from code-switched languages during the pandemic. Multimedia Tools and Applications pp. 1–17 (Jan 2022). https://doi.org/10.1007/s11042-021-11601-9
15. Rotemberg, V., Kurtansky, N., Betz-Stablein, B., Caffery, L., Chousakos, E., Codella, N., Combalia, M., Dusza, S., Guitera, P., Gutman, D., Halpern, A., Helba, B., Kittler, H., Kose, K., Langer, S., Lioprys, K., Malvehy, J., Musthaq, S., Nanda, J., Reiter, O., Shih, G., Stratigos, A., Tschandl, P., Weber, J., Soyer, H.P.: Publisher Correction: Author Correction: A patient-centric dataset of images and metadata for identifying melanomas using clinical context. Scientific Data **8**(1), 88 (Dec 2021). https://doi.org/10.1038/s41597-021-00879-x, http://www.nature.com/articles/s41597-021-00879-x
16. Sugeno, M., Murofushi, T.: Pseudo-additive measures and integrals. Journal of Mathematical Analysis and Applications **122**(1), 197–222 (Feb 1987). https://doi.org/10.1016/0022-247X(87)90354-4, https://linkinghub.elsevier.com/retrieve/pii/0022247X87903544
17. Tahani, H., Keller, J.: Information fusion in computer vision using the fuzzy integral. IEEE Transactions on Systems, Man, and Cybernetics **20**(3), 733–741 (Jun 1990). https://doi.org/10.1109/21.57289, http://ieeexplore.ieee.org/document/57289/
18. Tan, M., Le, Q.: EfficientNet: Rethinking model scaling for convolutional neural networks. In: Chaudhuri, K., Salakhutdinov, R. (eds.) Proceedings of the 36th International Conference on Machine Learning. Proceedings of Machine Learning Research, vol. 97, pp. 6105–6114. PMLR (09–15 Jun 2019), https://proceedings.mlr.press/v97/tan19a.html
19. Tiwari, A., Saha, S., Bhattacharyya, P.: A knowledge infused context driven dialogue agent for disease diagnosis using hierarchical reinforcement learning. Knowledge-Based Systems **242**, 108292 (2022). https://doi.org/https://doi.org/10.1016/j.knosys.2022.108292, https://www.sciencedirect.com/science/article/pii/S0950705122000971
20. Tschandl, P., Rosendahl, C., Kittler, H.: The HAM10000 dataset, a large collection of multi-source dermatoscopic images of common pigmented skin lesions. Scientific Data **5**(1), 180161 (Dec 2018). https://doi.org/10.1038/sdata.2018.161, http://www.nature.com/articles/sdata2018161